RETROFITTING OF SHEAR DEFICIENT INTERIOR SLAB-COLUMN CONNECTIONS IN RC FLAT-PLATES USING EPOXY RESINS

Zafar Iqbal Baig
Department of Civil and Environmental Engineering, Majmaah University, P.O. Box 66, Majmaah 11952, Saudi Arabia.
zbaig@mu.edu.sa

ABSTRACT: *This research reports the results of an experimental study on the use of epoxy resins as retrofitting material in the slab-column connections in reinforced concrete flat-plates subjected to concentric loading. Series of experimental tests are conducted on six isolated slab-column connections organized in two groups depending upon their compressive strength ranges. In each series, except for the control specimens, two different techniques for retrofitting of slab-column connections are considered. A constant flexural reinforcement ratio of 1.25% has been used for all the specimens to observe the effect of retrofitting techniques. The slab-column connection strengths are evaluated using ACI 318-11 code equations. From the test data obtained, the equations for interior slab-column connections under concentric loading as a function of concrete strength are developed. The results show that the retrofitting techniques used are effective in enhancing and restoring the load-carrying capacities from 12 to 30% relative to the control specimens.*

Keywords: punching shear, concentric, failure mode, slab-column, epoxies

1. BACKGROUND

Flat-plate and flat-slab floor systems are widely used in residential and commercial buildings. The flat-plate system is comparatively economical for use in buildings that do not have to accommodate large gravity loads. The addition of drop panels or column capitals permits for an increase in the gravity loading. In cases, where loads are relatively low and spans are moderate, it is possible to construct flat-plates with spans from 4.5 to 6 meters such that the slabs rest directly onto the columns (Figure-1a). Such structures have been used since the mid 20th century and are one of the most common floor systems employed in the construction of many multistory buildings such as offices, hotels, and apartments throughout the world because of their advantages such as flat ceilings, simplified formwork, and reduced story heights. In spite of numerous advantages, there also exit some disadvantages, for example, presence of high shear stresses in the slab-column connection regions due to negative bending moments and shear forces (Hueste and Wight, 1997; Megally and Ghali, 2000). To handle the high concentration of shear stresses, areas at the slab-column connection regions needs to be increased using drop panels, or column capitals (Figure-1b), but it gives complexity of the formwork.

Additionally, the slab-column connections in reinforced concrete flat-plates become under strength due to several reasons such as change of building use, need of installing new services, design and construction errors, or due to early removal of the shoring. In all these situations, the structures become susceptible to brittle failures in which slabs fail in a local area around the columns. Figure 2 illustrates a punching shear failure phenomenon occurring at an interior slab-column connection. The cracking occurring around the column perimeter is initially flexural followed by some successive circumferential cracks; causing separation of a truncated cone or pyramid-shaped concrete area from the main slab around the columns, called punching shear failure. Once the punching shear failure occurs, the overall resistance of the structure is considerably reduced. This type of failure sometimes may cause a progressive collapse of the entire floor or the entire structure. In such cases, the slab-column connections must be replaced or strengthened. The strengthening can be a cost-effective alternative to the replacement and is often the best solution. The choice of strengthening technique applied to any particular situation depends on the technical and economic factors and may be a complex task (Harajli and Soudki, 2003).

Background

The problem of punching shear failure at slab-column connections in the reinforced concrete flat-plates is being investigated by various researchers date backs to 1980. To overcome this problem many solutions have been suggested for example: removal and substitution of the damaged concrete (Pan and Moehle 1992; Ramos et al. 2000; Ospina et al. 2001); installation of shear bolts (El-Salakawy et al. 2003; Adetifa and Polak 2005), installation of steel collars (Iglesias, 1986), bonding of steel plates (Zhang, et al. 2001), stud shear reinforcements (Megally, S., and Ghali, A., 2000); and application of fiber reinforced polymers (Ebead and Marzouk, 2004; Esfahani et al. 2009). Most of the above-mentioned techniques emphases to avoid or delay punching failures. Some of them do provide enough additional strength to the slab-column connections; however, they are elaborate, difficult to install, expensive and aesthetically not pleasing. On the other hand, strengthening with epoxy resins used in this study is simple, does not require expensive labor and gives a pleasing appearance of the slab-column connections. To the best of authors' knowledge, no research has been conducted so far on retrofitting interior slab-column connections using epoxy resins under concentric loading.

Research significance

This research focuses on the retrofitting techniques in the existing reinforced concrete flat-plates built in the mid 20th century, which were commonly used as office or apartment buildings with the characteristics of no shear reinforcement or lack of concentration of the slab's flexural reinforcements over the columns (Figure-3). The intent of this research is to develop an effective retrofitting technique for reinforced concrete flat-plates with less labor involvement and without changing the appearance of the slab-column connections. With a further aim to develop an easily applied and convenient retrofitting that is non-intrusive on the existing available space.

Materials

Two series of analogous slab-column connections, detail of which is given in Table-1, were tested. The concrete compressive strength $(f_c^{'})$ equal to 14 and 28 MPa were selected to simulate low to reasonable concrete strength ranges, much like the reinforced concrete flat-plates built in

the mid 20th century. All the specimens were cast with concrete ordered from a local ready-mix concrete company. For each series of specimens, fifteen 150 x 300 mm concrete cylinders and nine 150 x 150 x 600 mm concrete beams were cast. Three out of fifteen concrete cylinders were standard cured to assertion the compressive strength of the supplied concrete whereas the remaining specimens (cylinders and beams) were cured and tested under similar conditions and ages as the relevant slab-column test specimens. The mechanical properties of the concrete such as compressive strength $(f_c^{'})$, modulus of elasticity $(\mathrm{E_c})$, and modulus of rupture (f_r), measured by the standard tests are listed in Table-1.

The steel reinforcement ASTM Grade 60 consisted of 20, 18 and 8 mm diameter deformed bars were used as longitudinal reinforcement in the stub columns, flexural reinforcement in the slabs, and stirrups in the stub columns respectively. Three rebars were tested from each type of steel reinforcement and the mechanical properties measured through uniaxial tension tests are enlisted in Table-2. The stress-strain curves obtained for tested steel reinforcement are shown in Figure-4.

Three different types of epoxy resins were used for retrofitting of the test specimens. Each epoxy resin served a specific purpose; for example, 1) thixotropic adhesive mortar based crack sealer epoxy resin was used to prevent leaking from slab bottom faces and around slab-column connections; 2) high strength based pourable grout epoxy resin was used to replace the spalled and damaged concrete in the slab-column connection regions, and 3) low viscosity based crack injection epoxy resin was used to fill the cracks. All the three products were from the Sikadur® and are shown in Figure 5. The properties of epoxy materials used are enlisted in Table-3.

Design and construction of test specimens

To conduct experiments on isolated slab-column connections, two series of specimens were formulated. Each series consisted of three specimens with slab dimensions of 2200 x 2200 x 150 mm^3 and column dimensions of 250 x 250 mm^2 representing interior slab-column connections. All the test specimens were identical in terms of shape, size, and reinforcement. The only difference was the concrete strength. Typical dimensions and layout of the tested specimens are shown in Figure-6. The drawings show the rebars as those were positioned for numerous existing structures built in the mid 20th century when the trend toward lighter and more flexible construction configurations led to the increased usage of flat-plate construction. One reference specimen in each series, simulating an existing reinforced concrete flat-plate connection requiring retrofitting has been named as control. The flexural reinforcement used in the slabs was determined according to the yield line theory which states that the bending moment remains constant along the yielding lines of the slab. The specimens were designed to fail in punching shear. Design calculations endorsed the use of 14-Ø18 rebars as the flexural reinforcement yielding reinforcement ratio, $\rho = 1.25\%$ with c/c spacing of 160 mm. The flexural reinforcement in the slabs was placed consisted of rebars running in North-South (N-S) and East-West (E-W) directions and tied together to form a single mat. The reinforcement placement in N-S and E-W directions was arranged such that the bars running in N-S direction gave the maximum depth, and the distance measured from the compression face of the slab to a layer midway between the centroid of the flexural reinforcement resulted in a slab effective depth of 112 mm. To provide a clear concrete cover of 20 mm to the flexural reinforcement running in N-S direction and to support the reinforcement running in both the directions, chairs made of Ø8 mm rebars were used. The steel chairs were placed away from the shear zones so that they do not act as slab shear reinforcement. Electrical strain gauges were attached to some of the rebars before their placement in the formwork and were run out on the sides of the formwork. Four lifting inserts, one in each corner of the slab specimens were installed while casting for shifting of the specimens.

For each test specimens, two square stub columns stubs with dimensions of 250 mm x 250 mm reinforced with 4-Ø20 bars as longitudinal reinforcement enclosed in Ø8 mm stirrups each spaced at 150 mm c/c was provided. The clear concrete cover to the stirrups in the column cage was 25 mm. The stub column was cast monolithically with the slabs and extended from both compression and tension faces of the slabs to simulate as closely as possible conditions and construction limitations that would exist in actual interior slab-column connections.

Test setup and instrumentation

A stiff reaction steel frame was used in the testing of the specimens. A 7.5-ton capacity crane was used to lift and install the test specimens inside the test frame. Prior to the testing, all the specimens were simply supported along all four edges to represent the region of the negative bending moment around an interior slab-column connection. The base of the lower stub column stub was placed on the load cell that was supported by a hydraulic jack of capacity 1000 kN and reacted by a strong test floor of the Structural Engineering Laboratory. To simulate the loading effects that the specimens would experience, a concentric vertical upward pressure was applied and increased monotonically until failure. The photograph of the test setup assembly used is shown in Figure-7.

The electrical resistance strain gages PL-60-11-5L (13), were used to measure strains in concrete on the compression faces of slabs as shown in Figure 8. Linear variable displacement transducers (LVDTs) were placed at various locations such as on the top of upper column stub, in the maximum shear stresses region and edges of the slabs. The position of LVDTs is shown in Figure-9. All the strain gauges, load cell and LVDT(s) were connected to the data logger to measure strains, loads and displacements respectively.

Testing procedure

The test specimens (control and retrofitted) were loaded concentrically through the lower stub columns as shown in Figure-7, until failure to estimate the loading capacity. The ultimate loads at the failure of FP-CON-1 and FP-CON-2 specimens were measured at 313 and 449 MPa, respectively. Based on an assumption that fifty percent of the ultimate load represents a level of load on a structure where retrofitting may be required, initial loads of 156.5 and 224.5 kN were applied to FP-EIR-1 and FP-EIR-2 specimens respectively prior to their strengthening. At this level of loading, due to low concrete strength, the FP-EIR-1 specimen experienced bending cracks followed by the flexural cracks on the tension face of the slab. No such

cracks in case of FP-EIR-2 specimen were observed, attributing to reasonable concrete strength; thus strengthening of FP-EIR-2 specimen by crack injection epoxy resin was not possible.

SPECIMENS' RETROFITTING

Several researchers have reported on previously failed and repaired slab-column connections using grouts to replace the damaged concretes. A rehabilitation method similar to this study was performed by Pan and Moehle (1992) and found that the use of epoxy repair helps to restore continuity of the discontinuous bottom reinforcement in slab-column connections.

Strengthening of FP-EIR Specimens

Using compressed air, top and bottom slab surfaces of the FP-EIR-1 specimen were cleaned and the cracks were blown out to remove any dust, debris or foreign particles. The widths of cracks occurring on the tension face of the slab were measured and found in the range of 0.2 to 5 mm. In order to prevent leaking through the slabs and around slab-column connection, the cracks were sealed using crack sealer epoxy resin, the properties of which are enlisted in Table-3. Using same crack sealer epoxy resin around the injection port-bases, the injection ports were installed 200 mm apart by placing directly over the crack, and bonding to the concrete surface. For each crack length, the porting was started at one end, until the entire crack length is ported. To avoid any leaking during injection of epoxy resin, the crack sealer was also mound about 5 mm thick and 25 mm wide around the injection ports and along the entire crack length leaving the port-holes uncovered (Figure-10). The paste-over was left for an overnight to cure for 24 hrs before injection of epoxy.

A two-component (Part A resin and Part B hardener), low viscosity gravity-fed, crack injection epoxy resin was decanted completely into a mixing bucket and was thoroughly mixed for three minutes using a slow running drill with a windmill type paddle (max. speed 600 rpm). The mixed crack injection epoxy resin was loaded in a locally fabricated epoxy injection pump (Figure 10). The epoxy injection pump also provided pressure readings during the injection. The nozzle of the epoxy injection pump was connected to the holes provided in the injection ports. The injection of the epoxy resin through entry ports was started at low pressure with the widest section first, from one end to the other and was continued until there was an appearance of epoxy resin at the adjacent entry port. The first entry port was plugged with the cap provided and then moved to the next port, repeating this procedure until the entire crack was filled with the epoxy resin. In some instances, the entry-ports injected previously showed accepting more epoxy resin while the injection was being done in the remaining ports. In this situation, the injection of epoxy resin in the remaining ports was suspended and injection was re-carried into the previously completed ports until it accepted no more epoxy resin. This process was repeated until every entry-port has refused epoxy resin. During injection, it extremely cared that no entry-port was left unattended. It was also noticed that moving to the next entry-port as soon as epoxy resin appears allowed the epoxy to travel along with the wider parts of the crack rather than forcing it into the crack. A time of three days was allowed for ambient curing and complete penetration of the epoxy resin into the cracks. The specimen was installed in the test set up and was tested under the same boundary conditions as the control specimen.

Repair of FP-ECR Specimens

The punching shear strength is often not explicitly addressed in a rehabilitation process. In this study, it was assumed that replacing spalled and damaged concrete with high strength pourable grout based epoxy resin will allow the repaired specimens to restore nearly the same punching shear strength as undamaged specimens.

The configuration of FP-ECR-1 and FP-ECR-2 specimens was similar to their companion specimens in shape, size, and reinforcement ratios. The specimens were first tested to failure, then repaired, and re-tested. Before they were repaired, both the specimens had failed in punching shear with severe cracking radially away from and concentrically around the columns. The spalling of concrete and pushing of the columns through the slabs all took place (Figure 11a). Removal of cement paste to expose the aggregate was required in the area of repair to establish sufficient bonding of epoxy resin to the slab concrete. All the damaged and spalled concrete in the connection regions was crushed using a chisel and hammer and was removed by hand. Using compressed air, the exposed surface of the broken concrete was cleaned and all loose particles were removed out (Figure 11b). In order to prevent leakage of the material, compression faces of the slabs and the column rounds were properly sealed using crack sealer epoxy resin. The paste-over were left for one day for sufficient hardening.

A three-component (Part A resin, Part B hardener, and Part C silica sand) pourable grout based epoxy resin was mixed as per manufacturer's instructions. Firstly, Parts A and B were mixed in a mixing bucket using a paddle attached to a slow speed drill (300-450 rpm), until the material became uniformly blended in color and viscosity. After complete mixing of parts A and B, the contents of component C as an aggregate were added and thoroughly mixed until uniform and homogeneous grout was obtained (Figure 12).

All the area obtained by removal of spalled and damaged concrete in the slab-column connection region was replaced using mixed pourable grout based epoxy resin of flowable consistency. The surface was made leveled and smooth by troweling and was left for three days for ambient curing. Fig. 11c shows a close-up view of slab top surfaces of FP-ECR specimens after repair. The repaired specimens were re-loaded until a second failure took place.

Estimated construction cost

The retrofitting cost of slab-column connections by crack sealer epoxy resin and by replacement of damaged concrete with high strength pourable grout epoxy resin are dependent on a number of factors, including access to the damaged concrete, concrete surface condition and volume of repair work to be performed. The estimates given here are intended only as an approximate reference for comparison with other possible repair techniques. Strengthening by crack sealer epoxy resin and by replacement of damaged concrete with high strength pourable grout epoxy resin such as performed in this study is estimated to cost $20 and $30 per square meter of slab area, respectively.

DISCUSSION OF TEST RESULTS

The test observations are described in terms of recorded deflections, loads, strains, and failure modes obtained for three specimens in each series.

Load-deflection response

To measure slabs deformations, linear variable displacement transducers (LVDTs) were installed at different locations on tension faces of the slabs. For each test specimen, the slab deflection was determined by taking the difference between deflection at the center of the slab and average deflection at the slab edges. Load-deflection diagrams, for series FP1 and FP2 specimens, are plotted in Figure 13. The load-deflection diagram of FP-CON-1 specimen shown in Figure 12a is characterized by brittle failure. This brittle failure attributed to low concrete compressive strength and heavily reinforced slab-column connection. The observed deflection of 30 mm at ultimate load in case of FP-CON-1 is lower than the deflections obtained in case of FP-ECR-1 and FP-EIR-1 specimens. It is observed that all the specimens in series FP1 failed in punching shear, as indicated by their load-deflection diagrams.

The load-deflection diagram of FP-CON-2 specimen exhibited a sharp peak followed by a significantly lower resistance and failed in punching shear prior to the formation of the yield-line mechanism because of the effect of heavy reinforcing bars. As shown in Figure 12b, the FP-ECR-2 specimen, reached the state of steadily increasing deflections at constant load, which is a normal characteristic for a reinforced concrete specimen experiencing flexural failure.

In general, the retrofitted specimens resulted in increased relative central deflections. The crack injection epoxy resin showed less effect on the central deflection compared to the high strength pourable grout epoxy resin. Table 2.6 summarizes the results of load-deflection measurements for all the specimens.

Ultimate load-carrying capacity

The ultimate load-carrying capacity will be referred to as the load capacity. The ultimate loads obtained for all the specimens are presented in Table 2 and Figure 12. The load capacity of specimen FP-CON-2 was 3% higher than that of specimen FP-CON-1. The ultimate loads increased by 7% for FP-ECR-1 and 11% for FP-EIR-1 specimens as a result of retrofitting compared with FP-CON-1 specimen. A similar trend was observed for specimen FP-ECR-2, retrofitted using high strength pourable grout epoxy resin that showed an increase of 40% in load capacity over that of FP-CON-2 specimen. The concrete strength used in the preparation of specimens of series FP1 was 14 MPa. It is also observed that as the concrete strength was increased from 14 to 28 MPa for specimens in series FP2, the ultimate load increased from 622 to 1363 kN. Hence, it can be concluded that the concrete strength had a strong influence on the punching shear capacity. The ultimate loads obtained for specimens FP-EIR-1 and FP-CON-2 are comparable, that the retrofitting technique in the former resulted in enhancing the load capacity of the under-strength specimen. The high strength pourable grout epoxy resin resulted in increasing the ultimate load in the range of 17 to 45%, whereas the crack injection epoxy resin resulted in increasing up to 28 % over the corresponding control specimens. It is observed that the retrofitting with high strength pourable grout epoxy resin is more effective for specimens with lower concrete compressive strength. The retrofitted specimens have not only carried higher loads but also sustained greater deflections till ultimate stage.

Stiffness characteristics

The stiffness of a slab at any loading point is the slope of the load-deflection curve at that point. In Figure 12, the initial tangents have been drawn and the point where the load-deflection response deviated from the initial elastic response gave an indication of the point of first cracking. From this Figure an increase of first cracking loads with increasing concrete strength has been observed which would be expected. The specimen FP-ECR-2 recorded a first crack load of 27.49 kN, which is the highest among other specimens. At initial behavior of the specimens, the central deflection has been decreased at a certain load level attributed to the increased stiffness of the specimens. The average initial stiffness of specimens FP-ECR-1 and FP-EIR-1 was about 2.37 times that of FP-CON-1. Moreover, the average initial stiffness of specimen FP-ECR-2 was about 1.99 times that of FP-CON-2. This may be attributed to the contribution of the retrofitting in increasing slab stiffness. The results show that the slab-column connections retrofitted with epoxy resins had stiffness and strength exceeding that of the control specimens. This agrees with the research results reported by Farhey et al. (1995) in which use of epoxy was effective to restore and even increase the strength, stiffness, and the ductility of the connection provided that the slab-column connection remains intact. Table 2.6 summarizes the results of load-deflection measurements for all specimens.

Energy absorption characteristics

The energy absorption is the area under the load-deflection curve for a tested specimen. The area of load-deflection curves given in Figure 12 was calculated numerically by the integration method. The calculated energy absorption values for tested specimens are presented in Table 4. The FP-CON-1 specimen has the energy capacity of 122.34 Joules which is lower than FP-CON-2 specimen. It was clearly noticed that the retrofitting technique contributed to an increase in the energy absorption of the retrofitted specimens compared with the control specimens. The FP-ECR-2 specimen has recorded the maximum energy absorption of 1426.71 Joules, which is higher than the other two slab specimens i.e. FP-ECR-1 (623.98 Joules) and FP-EIR-1 (694.86 Joules). The increase of energy absorption capacity of FP-ECR-2 specimen is about 410 to 1066% and 9654 to 22202% when compared with FP-CON-1 and FP-CON-2 specimens respectively. Hence, it can be concluded that the high strength pourable grout epoxy resin retrofitted specimens show superior performance than the crack injection epoxy resin retrofitted specimens.

Strain measurements

Figure 14 shows the measurements made to determine the steel strain distribution for flexural reinforcement at several locations. The horizontal line in this Figure illustrates the average yield strain of the reinforcing bars, determined as 2500με from uniaxial tension tests (Table 3). The measured steel strain of 0.01 for FP-ECR-2 specimen indicates that yielding of flexural reinforcement exceeded from the average yield strain of the reinforcement. This yielding of flexural reinforcement occurred at the column face and the steel strain at failure load was approximately four times the yield strain. In case of other specimens in both the series, the steel strain recorded during testing ranged between 0.001 and 0.01 indicating that for these specimens, the steel strain did not reach the yield strain at the failure loads and failure took place without yielding of the reinforcement.

Table 3 shows description of yielding in the flexural reinforcement.

The concrete strain profile was measured on the compression faces of the tested specimens to observe the strain levels during the loading. The horizontal line in Figure 15 illustrates the average value of concrete strain at crushing taken as 3000με. The measured compressive strain ranged between 2 and 938με indicating that crushing of concrete on the compression faces of the slabs did not occur in any of the specimens. The measurement of very low compressive strain in all the specimens suggests that failure was of the shear-compression type.

Cracking and failure patterns

The crack patterns of tested specimens are presented in Figures 15 to 17. It can be observed from these Figures that the crack pattern is almost similar in all the retrofitted specimens.

For specimen FP-ECR-2, the flexural reinforcement yielded and showed relatively large deflection values before reaching the ultimate load. All the specimens except FP-ECR-2 showed brittle modes of failure due to punching shear. Figure 16 shows the cracking pattern of the control specimens, FP-CON-1 & FP-CON-2.

The typical brittle failure modes of FP-ECR-1 and FP-EIR-1, retrofitted specimens are shown in Fig. 17 and 18, respectively. It is evident that the epoxy resins contributed to an increase in the load capacity. These cracks were located along the edges of the strengthening material length. After the appearance of these cracks, the specimens failed due to accelerated concrete flexural failure.

The remaining slab-column connections, FP-ECR-1 and FP-EIR-1, clearly failed in pure punching long before their flexure strength was reached. The punching-shear surface on the tension face occurred at a distance of 1.2 to 1.6 times slab depth *d* from the column face for most of the tested specimens.

The punching shear surface on the tension face occurred at a distance of 1.2 to 1.6 times slab depth *d* from the column face for most of the tested slabs. The failure surfaces of a few tested specimens were caredful1y removed and examined. The observed angles of failure surface varied considerably.

For the FP-ECR-2, the crack pattern observed prior to punching consisted of one tangential crack, roughly at the column outline, followed by radial cracking extending from the column. Yet punching failure occurred before the flexure yield lines were well developed. This failure can be classified as flexure-punching or secondary shear failure. For the slabs failing by punching shear, the cracks were first formed tangentially under the edge of the column stub, followed by radial cracking extending from the column. The first radial cracks were much more pronounced along the lines parallel to the reinforcement passing through the column stub. As the load was increased, the tangential cracks were then extended outside the circumference of the stub column. Those tangential cracks were limited to the column vicinity. The slabs failed with the final shear crack coinciding with or located outside, this crack. Final failure developed by the column punching through the slab

.

Table 1: **Detail of tested specimens and concrete properties**

Title	Description		Compressive Strength, $f_c^{'}$ (MPa)	Modulus of Elasticity, E_c (GPa)	Modulus of rupture, f_r (MPa)
FP-CON-1	Slab depth, h = 150 mm Effective slab depth = 112 mm Reinforcement ratio = 1.5% Compressive strength = 14 MPa	Control	16.1	13.3	2.92
FP-EIR-1		Strengthened	16.7	12.9	2.84
FP-ECR-1		Repaired	16.5	14.1	2.69
FP-CON-2	Slab depth, h = 150 mm Effective slab depth = 112 mm Reinforcement ratio = 1.5% Compressive strength = 28 MPa	Control	29.4	23.6	4.19
FP-EIR-2		Strengthened	28.9	24.3	4.24
FP-ECR-2		Repaired	29.1	22.7	3.88

Table 2: Mechanical properties of tested reinforcement

Property	Nominal diameter		
	(8 mm)	(18 mm)	(20 mm)
Yield strength, MPa	522.290	433.096	468.520
Ultimate strength, MPa	642.720	654.809	648.906
Strain at yielding, mm/mm	0.00390	0.00232	0.00244
Strain at ultimate, mm/mm	0.08344	0.15024	0.14631
Modulus of elasticity, MPa	181,000	196,000	209,000

Table 3: Typical properties of cured epoxy resins†

Property	Crack sealer epoxy resin*	Pourable grout epoxy resin**	Crack injection epoxy resin***
Compressive strength, MPa	60-70	80	53
Flexural strength, MPa	30-40	30-35	50
Tensile strength, MPa	19-25	10-15	25
Adhesion on concrete, MPa Adhesion on steel, MPa	4 13-17	4 15-20	4 10
Shear strength, MPa	-	28.2	29.6
Modulus of elasticity, GPa	5	14	1.06
Viscosity, mPas	-	-	130
Elongation at break, %	0.4±0.1	-	-

†Manufacturer's reported values * Sikadur 31 **Sikadur 42 ***Sikadur 52

Table 4. Predicted and measured strengths of the tested specimens

Specimen's		Concrete strength, $f_c^{'}$ (MPa)	Predicted strengths (MPa)			Measured ultimate load, P_u (kN)	$\frac{P_u}{V_{flex}}$
Designation	Description		V_n	V_{flex}	V_n / V_{flex}		
FP-CON-1	Control	15.8	209	392	0.53	341	0.87
FP-EIR-1	Strengthened	17.1	-	-	-	472	1.20
FP-ECR-1	Repaired	16.6	-	-	-	385	0.98
FP-CON-2	Control	30.4	296	457	0.65	416	0.91
FP-EIR-2	Strengthened	29.7	296	457	0.65	-	-
FP-ECR-2	Repaired	30.9	296	457	0.65	481	0.98

Table 5. Deflection characteristics of tested specimens

Specimen's designation	First crack		Yield		Ultimate		Stiffness, k (kN/mm)	Failure Mode
	load, P_c (kN)	deflection, Δ_c (mm)	load, P_y (kN)	deflection, Δ_y (mm)	load, P_u (kN)	deflection, Δ_u (mm)		
FP-CON-1	98.0	1.88			341	11.3	28.3	Punching Shear
FP-EIR-1	76.7	0.92			472	13.0	26.0	Flexure
FP-ECR-1	60.0	0.09			385			Punching Shear
FP-CON-2			205.7	5.0	340.3	13.4	29.6	2.68
FP-EIR-2			256.3	8.1	359.3	16.3	29.5	2.01
FP-ECR-2			251.5	8.4	335.3	15.7	31.0	1.86

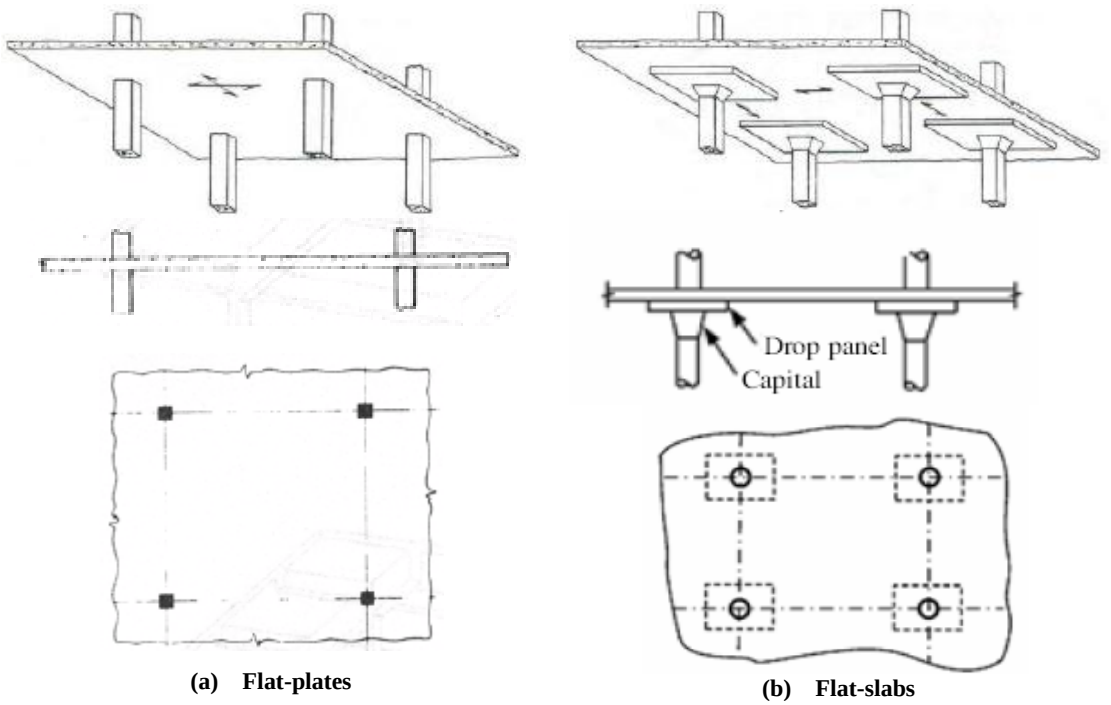

(a) Flat-plates **(b) Flat-slabs**

Figure-1: Reinforced concrete two-way slab structures

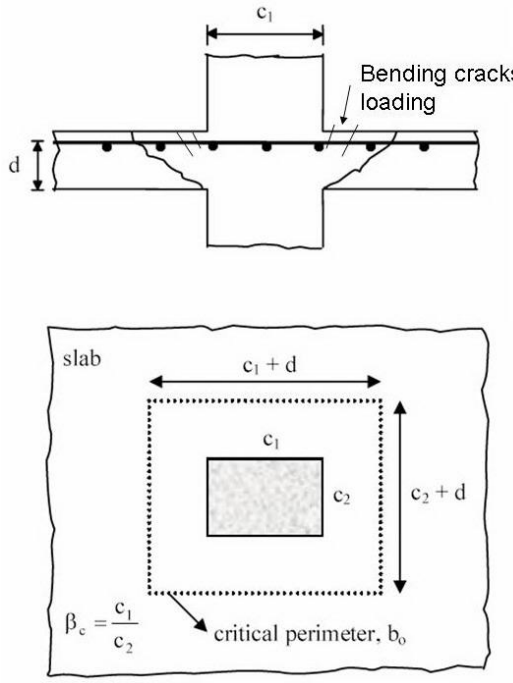

Figure-2: Illustration of punching shear failure at the slab-column connection

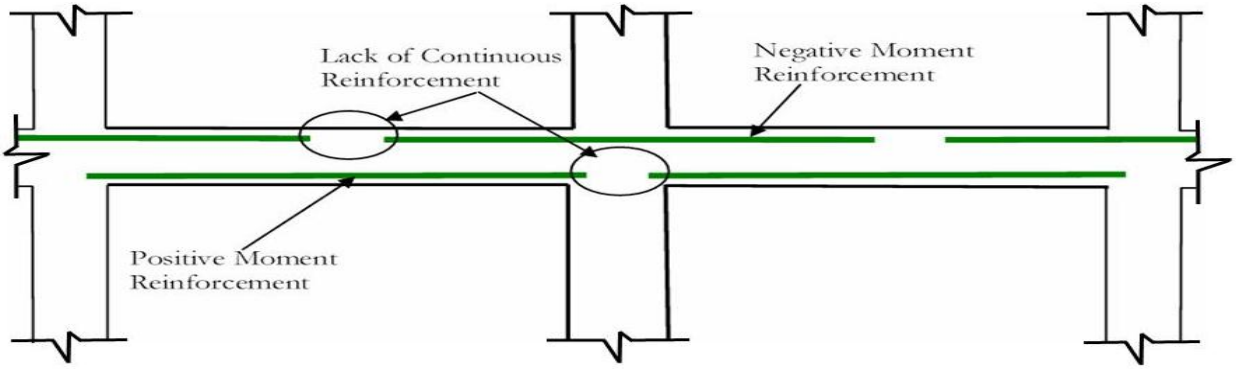

Figure-3: Lack of continuous reinforcement across RC structures

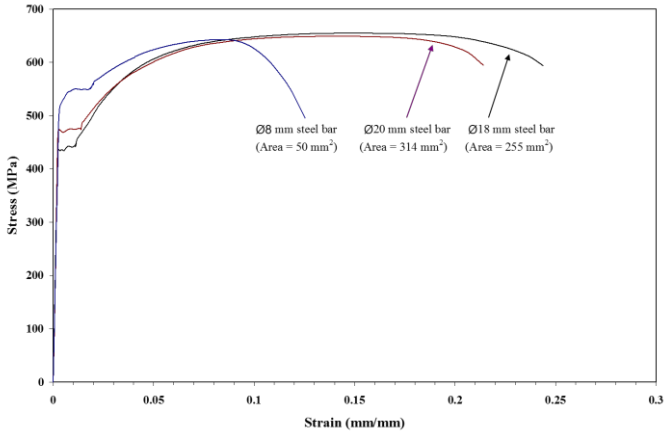

Figure-4: Stress-strain curves of tested reinforcement

(a) Sikadur 31 **(b) Sikadur 52** **(c) Sikadur 42**

Figure-5: Epoxy resins produced by Sikadur®, Swiss.

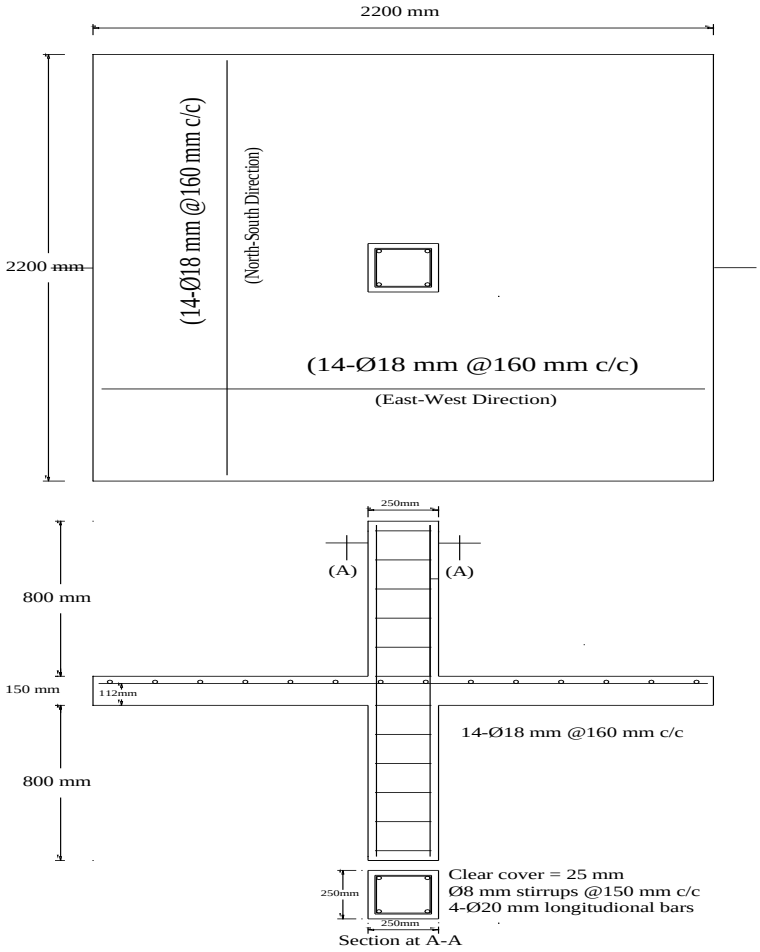

Figure-6: Typical dimensions and reinforcement details of tested specimens

Figure-7: Overall view of test setup assembly with the specimen.

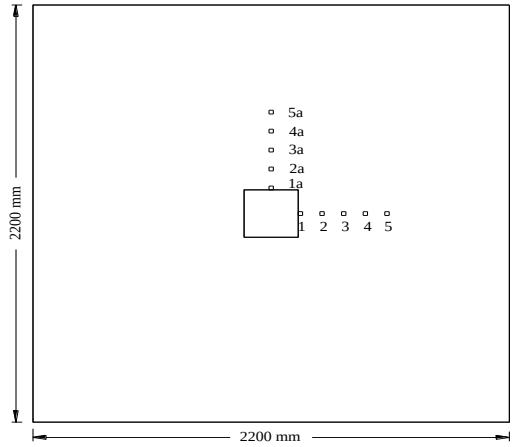

Figure-8: Location of electrical resistance strain gauges

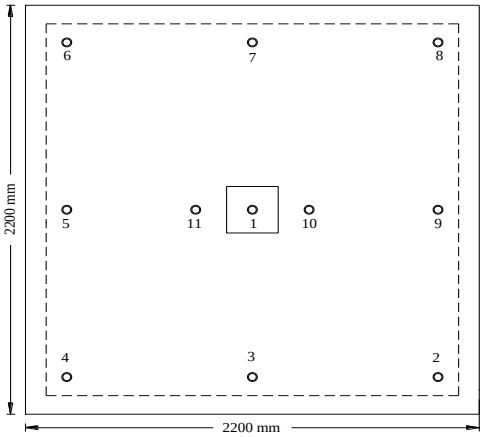

Figure-9: Location of linear variable displacement transducers (LVDTs)

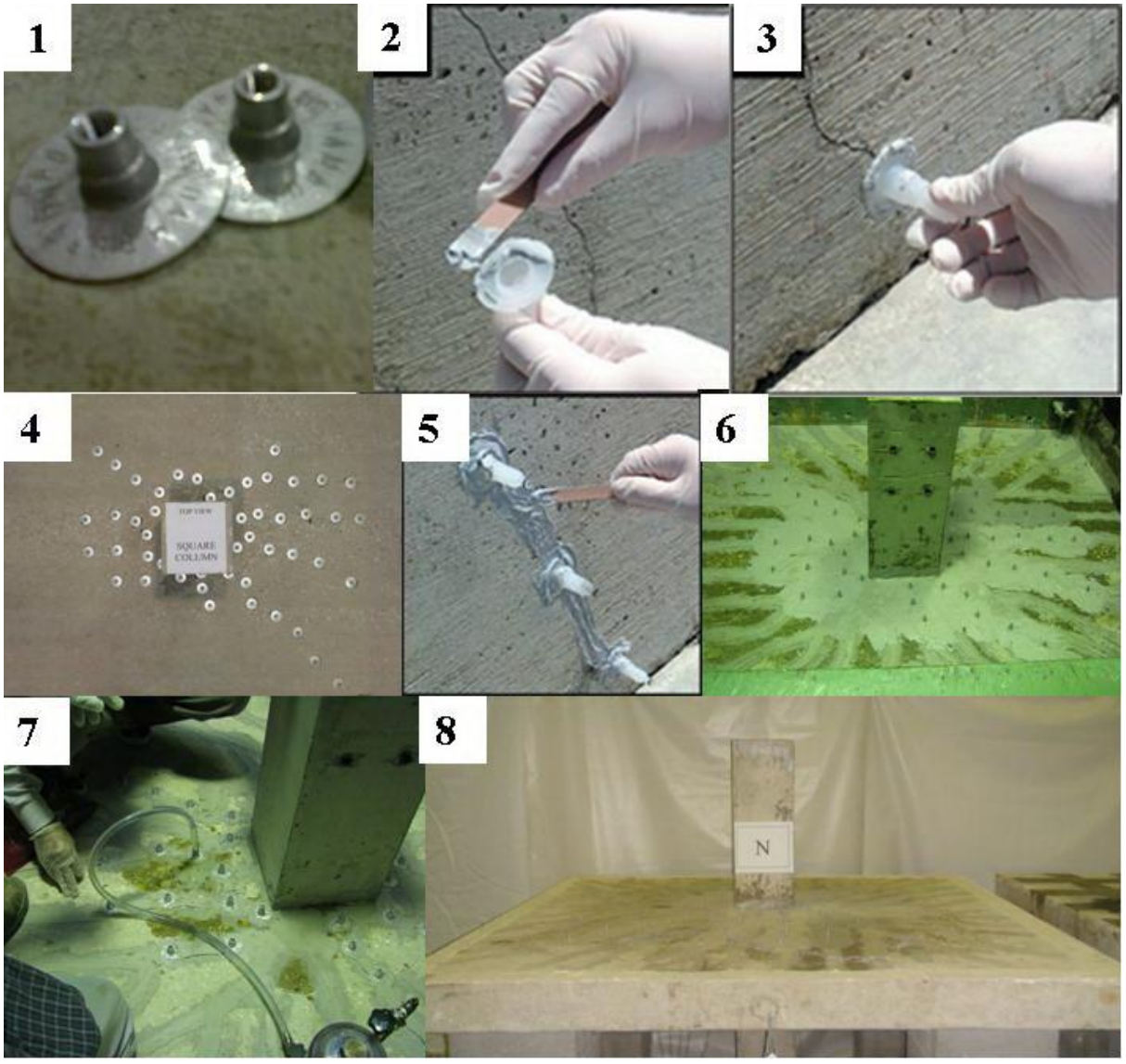

Figure-10: Strengthening process of FP-EIR specimens

FP-ECR-1 **FP-ECR-2**

(a) Specimens at first testing

FP-ECR-1 **FP-ECR-2**

(b) Specimens at the removal of damaged concrete

FP-ECR-1 **FP-ECR-2**

(b) Specimens after repair

Figure-11: Testing and repairing process of FP-ECR specimens

Figure-12: Mixing of high strength pourable grout epoxy resin

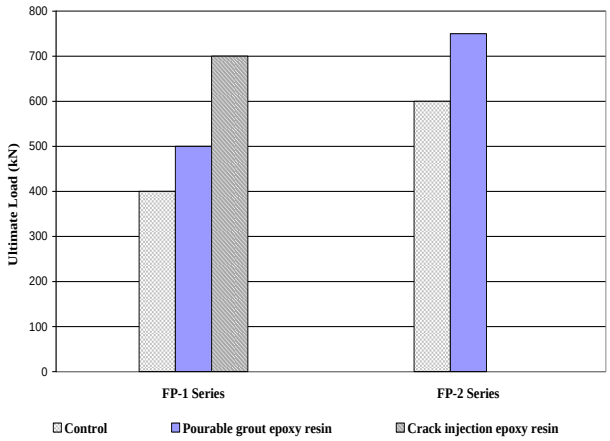

Figure-13: Comparative increase in the ultimate loads

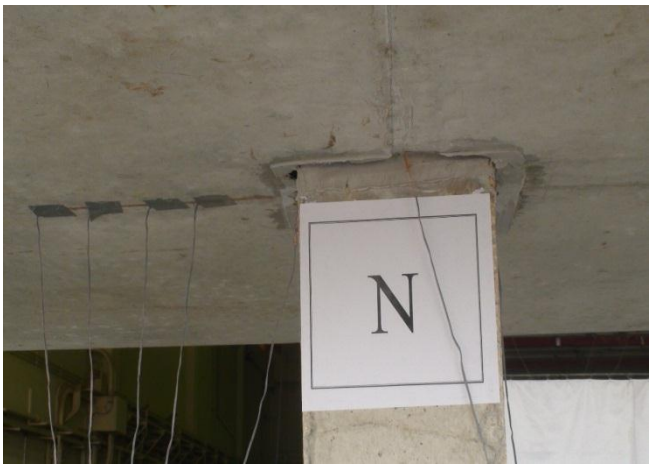

Figure-14: Comparative increase in the ultimate loads

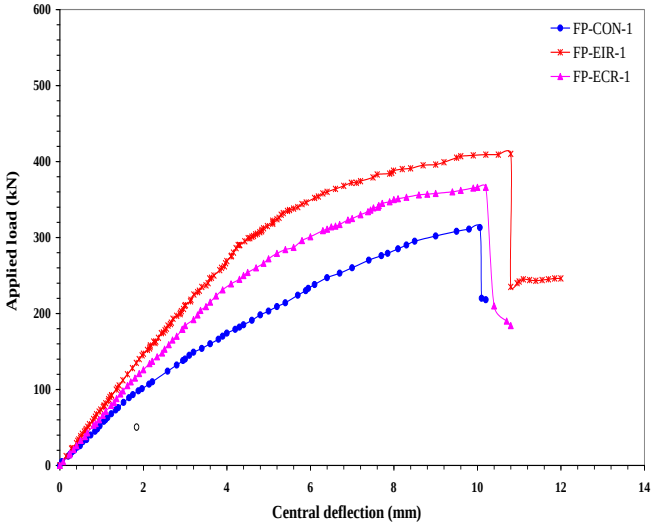

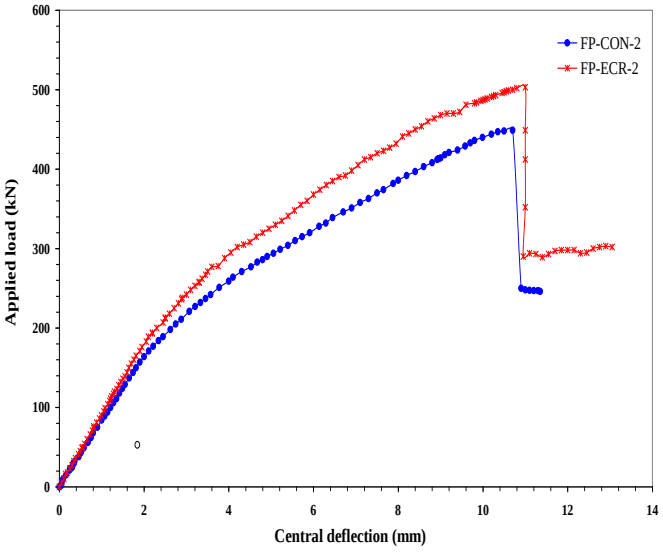

Figure-15: Comparative increase in the ultimate loads

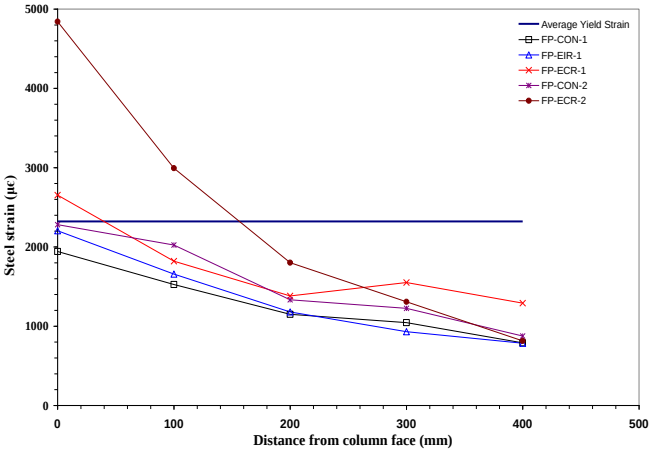

Figure-16: Steel strain distribution for flexural reinforcement

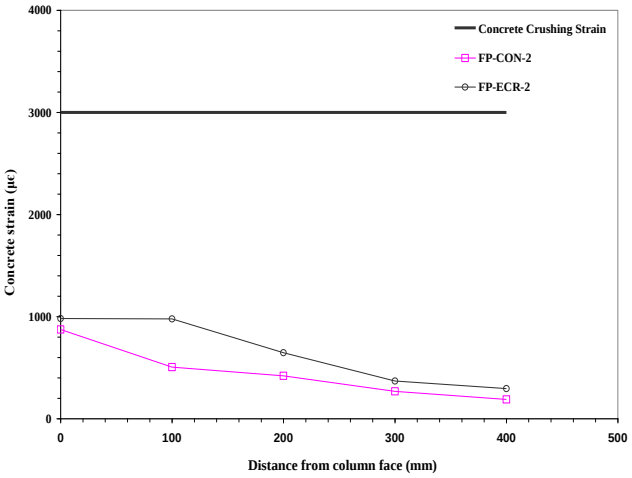

Figure-17: Comparative increase in the ultimate loads

It was not possible to determine a reliable value for the shear cracking load, i.e., the load at which the shear cracks began to open up because there was no fundamental difference between the shear cracks and flexural cracks running in a tangential direction. However, as proposed by Kinnunen and Nylander,3 utilizing the decrease of the strains in the flexure reinforcement as a guide for determining the shear-cracking loads, the observed shear-cracking loads were always greate-r than 70 percent of the ultimate load.

Post-punching behavior was monitored in some of the tests. When punching occurred, the load fell suddenly to a value of approximately 20 percent of the ultimate load and was released completely in some cases. With the further application of the load, a flat plateau of resistance was reached. The final failure progressed with the bottom bars being pulled out of the concrete.

CONCLUSIONS

The base specimen failed due to punching shear generated from the gravity loading. The four other types of retrofitted specimens using epoxy resins were shown to be efficient in resisting punching shear in the connections under gravity loading. Six interior slab-column connections were tested to failure. Based on the observed behavior and test results, the following conclusions were drawn:

REFERENCES

1. Hueste, M. B. D. and Wight, J. K., (1997). "Evaluation of a Four-Story Reinforced Concrete Building Damaged During the Northridge Earthquake", Earthquake Spectra, Vol. 13 (3), pp. 387-414.
2. Megally, S. and Ghali, A., (2000). "Seismic Behavior of Slab-column Connections". Canadian Journal of Civil Engineering, Vol. 27 (1), pp. 84-100.
3. Harajli, M. H. and Soudki, K. A., (2003). "Shear strengthening of interior slab-column connections using carbon fiber-reinforced polymer sheets". Journal of Composites for Construction, Vol. 7 (2), pp. 145–153.
4. Pan, A. D. and Moehle, J. P., (1992). "An Experimental Study of Slab-column Connections." ACI Structural Journal, Vol. 89 (6), pp.626-638.
5. Ramos, A. M. P.; Lucio, V. J. G. and Regan, P. E., (2000). "Repair and Strengthening Methods of Flat Slabs for Punching". Proceedings of the International Workshop on Punching Shear Capacity of RC Slabs, Stockholm, Sweden, TRITA-BKN: Bulletin 57, pp. 125-133.
6. Ospina, C. E.; Alexander, S. D. B. and Cheng, J. J. R. (2001). "Behavior of concrete slabs with fibre-reinforced polymer reinforcement." Structural Engineering Report No. 242, Department of Civil and Environmental Engineering, University of Alberta, Edmonton.
7. El-Salakawy, E. F.; Polak, M. A., and Soudki, K. A., (2003). "New Shear Strengthening Technique for Concrete Slab-Column Connections." ACI Structural Journal, Vol. 100 (3), pp. 297-304.
8. Adetifa, B. and Polak, M. A., (2005). "Retrofit of Slab Column Interior Connections using Shear Bolts". ACI Structural Journal, Vol. 102 (2), pp. 268-274.
9. Iglesias, J. (1986). "Repairing and Strengthening of Reinforced Concrete Buildings Damaged in the 1985 Mexico City Earthquake." The Mexico Earthquakes – 1985: Factors Involved and Lessons Learned, Proceedings of the International Conference, September 19-21, edited by Cassaro, M.A. and Romero, E.M., ASCE, New York, pp. 426-439.
10. Zhang, J.W.; Teng, J.G.; Wong, Y.L., and Lu, Z.T., (2001). "Behavior of Two-Way RC Slabs Externally Bonded with Steel Plate". Journal of Structural Engineering, Vol. 127 (4), pp. 390-397.
11. Ebead, U., and Marzouk, H., (2004). "Fiber-Reinforced Polymer Strengthening of Two-Way Slabs". ACI Structural Journal, Vol. 101 (5), pp. 650-659.
12. Esfahani, M.R.; Kianoush, M.R., and Moradi, A. R. (2009). "Punching shear strength of interior slab column connections strengthened with carbon fiber reinforced polymer sheets". Engineering Structures, Vol. (31), pp. 1535-1542.
13. Chen, C. C., and Li, C. Y., (2000). "An experimental study on the punching shear behavior of RC slabs". Proceedings of the International Workshop on Punching Shear Capacity on RC Slabs, Stockholm, pp. 415-422.
14. Ichimasu, H., Maruyama, M., Watanabe, H., and Hirose, T. 1993a. RC slabs strengthened by bonded carbon FRP plates: Part 1 - Laboratory study. International Symposium on Fibre Reinforced Polymer Reinforcements for Concrete Structures, ACI, Special Publication SP-138, pp. 932–955.
15. Ichimasu, H., Maruyama, M., Watanabe, H., and Hirose, T. 1993b. RC slabs strengthened by bonded carbon FRP plates: Part-2 Application. International Symposium on Fibre Reinforced Polymer Reinforcements for Concrete Structures, ACI, Special Publication SP-138, pp. 957–971.
16. Karbhari, V.M., Seible, F., Seim, W., and Vasquez, A. 1996. Poststrengthening of concrete slabs. International Symposium on Fibre Reinforced Polymer Reinforcements for Concrete Structures, ACI, Special Publication SP-188, pp. 1163–1173.
17. MacGregor, J. G., (1997). "Reinforced Concrete: Mechanics and Design". Prentice Hall, Upper Saddle River, N.J., 939 pages.

18. Moehle, J. P., (1986). "Seismic Response of Slab-column Frames", Proceedings of the Third U.S. National Conference on Earthquake Engineering, Charleston, SC, Vol.2., pp. 1505-1516.
19. Penelis, G. G. and Kappos, A. J., (1997). "Earthquake Resistant Concrete Structures". E & FN Spon, London.
20. Tokyo Sokki Kenkyujo Company, LTD, Minami-Shinagawa-KU, Tokyo, Japan.
21. Megally, S., and Ghali, A., (2000), "Seismic Behaviour of Edge Column-Slab Connections with Stud Shear Reinforcement", *ACI Structural Journal*, Vol. 97 (1), pp. 53-60.